

Published in final edited form as:

FASEB J. 2007 August ; 21(10): 2510–2519. doi:10.1096/fj.06-8070com.

Magnetically driven plasmid DNA delivery with biodegradable polymeric nanoparticles

Michael Chorny^{*,1}, Boris Polyak^{*,1}, Ivan S. Alferiev^{*}, Kenneth Walsh[†], Gary Friedman[‡], and Robert J. Levy^{*,2}

^{*}Division of Cardiology Research, The Children's Hospital of Philadelphia, Philadelphia, Pennsylvania, USA

[†]The Whitaker Cardiovascular Institute, Boston University School of Medicine, Boston, Massachusetts, USA

[‡]Drexel University School of Biomedical Engineering and Health Sciences, Philadelphia, Pennsylvania, USA

Abstract

Targeting gene therapy remains a challenge. The use of magnetic force to achieve this was investigated in the present study. It was hypothesized that nanoparticles with both controllable particle size and magnetic properties would enable magnetically driven gene delivery. We investigated this hypothesis by creating a family of novel biodegradable polymeric superparamagnetic nanoparticle (MNP) formulations. Polylactide MNP were formulated using a modified emulsification-solvent evaporation methodology with both the incorporation of oleate-coated iron oxide and a polyethylenimine (PEI) oleate ion-pair surface modification for DNA binding. MNP size could be controlled by varying the proportion of the tetrahydrofuran cosolvent. Magnetically driven MNP-mediated gene transfer was studied using a green fluorescent protein reporter plasmid in cultured arterial smooth muscle cells and endothelial cells. MNP-DNA internalization and trafficking were examined by confocal microscopy. Cell growth inhibition after MNP-mediated adiponectin plasmid transfection was studied as an example of a therapeutic end point. MNP-DNA complexes protected DNA from degradation and efficiently transfected quiescent cells under both low and high serum conditions after a 15 min exposure to a magnetic field (500 G). There was negligible transfection with MNP in the absence of a magnetic field. Larger sized MNP (375 nm diameter) exhibited higher transfection rates compared with 185 nm- and 240 nm-sized MNP. Internalized larger sized MNP escaped lysosomal localization and released DNA in the perinuclear zone. Adiponectin plasmid DNA delivery using MNP resulted in a dose-dependent growth inhibition of cultured arterial smooth muscle cells. It is concluded that magnetically driven plasmid DNA delivery can be achieved using biodegradable MNP containing oleate-coated magnetite and surface modified with PEI oleate ion-pair complexes that enable DNA binding.

Keywords

GFP plasmid; magnetic nanoparticles; ion-pair complex; polyethylenimine; adiponectin

© FASEB

²Correspondence: The Children's Hospital of Philadelphia, Abramson Research Bldg., Ste. 702, 3615 Civic Center Blvd., Philadelphia, PA 19104-4318, USA. levyr@email.chop.edu.

¹These authors contributed equally to this work.

The efficiency of nonviral gene delivery critically depends on providing an optimal local concentration of plasmid DNA in the target tissue and overcoming a number of barriers, including rapid degradation by extra- and intracellular endonucleases (1, 2) and restricted nuclear entry in nondividing cells (3, 4). Previous research by others has demonstrated that iron oxide nanoparticles with polyethylenimine (PEI) can be used for magnetically driven plasmid DNA delivery in cell culture (5, 6). However, despite promising results showing high gene transfer rates in some cell types under optimized conditions, inefficient transfection was demonstrated with this approach in association with toxicity in contact inhibited cells (7). Furthermore, iron oxide nanoparticle aggregation on DNA complexation in salt-containing medium resulting in a loss of colloidal stability (8–10) is also a limitation of this prior formulation. The present investigation pursued a DNA delivery concept combining a biodegradable polymeric carrier with magnetic targeting. It was hypothesized that polylactide (PLA)-based magnetic nanoparticles (MNP) formulated with incorporated iron oxide and surface modified with PEI as an oleate ion-pair complex could be used for magnetically driven gene vector delivery in cultured vascular cells in both low and high serum conditions. We also hypothesized that the following advantageous features would result: 1) controllable particle size determining both magnetic properties and cell trafficking; 2) efficient particle surface modification with PEI due to an oleate ion pairing strategy; 3) both high DNA binding capacity and protection in the presence of serum due to MNP-DNA complexation; and 4) efficient MNP-DNA complex cellular uptake and gene transfer after magnetic field exposure.

The goals of the present studies were to develop a novel formulation approach for preparing biodegradable nanoparticles with controllable size suitable for magnetically driven nonviral gene transfer. This approach was applied to create a family of PEI surface-coated, PLA-based MNP impregnated with iron oxide (Fig. 1), which were further characterized with respect to their magnetic properties, efficiency of PEI surface modification and DNA binding. We also studied the DNA delivery characteristics of these MNP in contact-inhibited cultured arterial smooth muscle and endothelial cells in terms of their dependence on particle size and serum conditions. We examined MNP intracellular trafficking and DNA release using confocal microscopy, and investigated the MNP-mediated delivery *in vitro* of a candidate therapeutic gene adiponectin for its effects on proliferation of PDGF-BB-stimulated smooth muscle cells.

MATERIALS AND METHODS

Materials

Enhanced GFP-encoding plasmid was obtained from Clontech (Mountain View, CA, USA). A human adiponectin-encoding plasmid was kindly provided under a material transfer agreement from Boston University (Boston, MA, USA). Both vectors were under the control of the human CMV promoter. Enhanced GFP plasmid without a promoter was provided by Dr. McCaffrey from the George Washington University (Washington, DC, USA). Poly(D,L-lactide) (M_r 75,000–120,000), ferric chloride hexahydrate, ferrous chloride tetrahydrate, sodium hydroxide, oleic acid, and branched polyethylenimine (PEI25 with the number molecular weight average ~10,000 according to the manufacturer's specifications) were obtained from Sigma-Aldrich (St. Louis, MO, USA). Succinimidyl esters of BODIPY FL, BODIPY 650/665, 7-diethylaminocoumarin-3-carboxylic acid, Lysotracker Red DND-99, and PicoGreen were from Molecular Probes (Eugene, OR, USA). CyTM 5 DNA labeling kit (Label IT[®] TrackerTM) was from Mirus Bio Corporation (Madison, WI, USA). All solvents were of HPLC grade. Deionized water used in all experimental procedures was obtained using a Milli-Q water purification system (Millipore, Bedford MA, USA). Before its use, PEI25 was dialyzed against deionized water using a membrane with 1000 Da cutoff.

Nanoparticle formulation

Magnetite obtained from ferric and ferrous chloride (65 mg and 33 mg, respectively) by alkaline precipitation with aqueous sodium hydroxide was magnetically separated, resuspended in 2 ml of ethanol, and coated with oleic acid (100 mg) with heating under argon to 90°C in a water bath for 5 min. Excess oleic acid was phase-separated by dropwise addition of 4 ml of water and the lipid-coated magnetite was washed twice with ethanol. Lipophilic magnetite was dispersed in a 6 ml organic solvent mixture of chloroform and tetrahydrofuran (THF) at different volume ratios, forming a stable magnetic fluid further used for the nanoparticle preparation.

PLA-based magnetite-loaded MNP were prepared by a modification of the emulsification-solvent evaporation method (12). Typically, 100 mg of oleic acid, 75 mg of PEI25, and 200 mg of PLA covalently labeled with BODIPY 650/665 were dissolved in 6 ml of magnetic fluid obtained as above to form an organic phase. The organic phase was emulsified in 15 ml of water by sonication and the organic solvents were removed by evaporation under reduced pressure at 30°C. The obtained particles were passed through a 1.0 µm glass fiber prefilter (Millipore, Bedford, MA USA), dialyzed against 4 l of water with several water replacements for 24 h using a dialysis membrane with a 300,000 Da cut-off (Spectrum Laboratories, Inc., Rancho Dominguez, CA, USA) to remove unbound PEI, and lyophilized with 10% (w/v) glucose as a cryoprotectant. Lyophilized MNP were kept at -20°C and resuspended in deionized water before use.

MNP characterization

Particle size and zeta potential measurements were performed using 90 Plus Particle Size Analyzer (Brookhaven Instruments, Holtsville, NY, USA). The magnetic properties of MNP were estimated from the hysteresis curves of 5 µl samples (corresponding to 125 µg) air-dried on a 4 × 4 mm² coverglass slide using an alternating gradient magnetometer (Princeton Instruments Corporation, Princeton, NJ, USA).

The iron content of MNP was determined spectrophotometrically in 1 N hydrochloric acid ($\lambda=335$ nm) against a standard curve after MNP degradation with 1N aqueous sodium hydroxide (90°C, 30 min) and dissolving the iron-containing precipitate in the acid solution.

The amount of MNP-associated PEI was determined fluorimetrically ($\lambda_{ex}/\lambda_{em}=420$ nm/475 nm) using MNP formulated with 7-diethylaminocoumarin-labeled PEI. A 100 µl aliquot of MNP was centrifuged, the supernatant was removed, and the pellet was resuspended in water. The PEI amount was determined against a standard curve of 7-diethylaminocoumarin-labeled PEI spiked with equivalent amounts of nonfluorescent MNP for background correction.

DNA binding by MNP was determined fluorimetrically ($\lambda_{ex}/\lambda_{em}=485$ nm/530 nm) using the PicoGreen assay adapted for a 96-well plate format (13). Plasmid DNA was diluted with MES buffer (0.1 M, pH 6.5) to a 2.0 µg/ml solution. A stock MNP suspension (60 µg of MNP in 1.0 ml of water) was serially diluted 1.25-fold, and the dilutions were mixed with equal volumes of DNA solution (50 µl) and incubated for 30 min at room temperature. Finally, the samples were incubated for 10 min with 100 µl of PicoGreen solution diluted 1:200. Samples containing no particles or no DNA were used as a reference and for background correction, respectively. The fraction of DNA bound to MNP was calculated using the formula $(F_{reference} - F_{formulation})/F_{reference} \times 100\%$, where F is the fluorescence of a respective sample.

Cell transfection and growth inhibition studies

Rat aortic smooth muscle cells (A10) and bovine aortic endothelial cells (BAEC) were seeded on clear-bottom 96-well plates at a density of 10^4 and 1.5×10^4 cells/well, respectively, for GFP reporter expression studies. A10 were seeded at 3×10^3 cells/well for cell growth inhibition studies after adiponectin gene transfer. DMEM supplemented with 10% fetal bovine serum (FBS) or 2% FBS and 10 ng/ml PDGF-BB were used as a cell culture medium for transfection and growth inhibition experiments, respectively. Plasmid DNA was incubated for 30 min with MNP at various ratios in 5% w/v glucose solution, diluted 5-fold with serum-containing DMEM to provide a final serum concentration of 10% or 50% (low and high serum conditions, respectively), and applied to cells at 0.25 μ g DNA/well. Cells were incubated with MNP-DNA complexes using a magnetic separator adapted for 96-well plates as a magnetic field source (LifeSep™ 96F, Dexter Magnetic Technologies, Fremont, CA, USA), then washed with PBS, and the medium was replaced with fresh DMEM supplemented with 10% serum. Cells treated with MNP-DNA complexes in the absence of magnetic field were used as a control. Fluorimetric measurements of MNP uptake ($\lambda_{ex}/\lambda_{em}=620$ nm/670 nm) and GFP expression ($\lambda_{ex}/\lambda_{em}=485$ nm/535 nm) were performed in live cells after 24 h and 48 h, respectively. Cell viability and cell growth inhibition were determined 72 h post-treatment using the AlamarBlue assay ($\lambda_{ex}/\lambda_{em}=540$ nm/575 nm) as described by the manufacturer (Biosource, Camarillo, CA USA) using untreated cells as a reference. All cell culture experiments were carried out in triplicate.

MNP cellular localization

MNP uptake and intracellular localization were studied using Leica DM IRE2 confocal microscope interfaced with a Leica TCS SP2 spectral confocal system/UV (Leica Microsystems, Wetzlar, Germany). DNA was labeled with Cy™ 5 dye according to the manufacturer's protocol. Cells were seeded on sterile glass-bottom dishes (35 \times 10 mm²) from Electron Microscopy Sciences (Fort Washington, PA, USA) at a density 10^5 cells/dish. One hour before applying MNP-DNA complexes, cells were pretreated with LysoTracker Red at a concentration of 50 nM in DMEM medium supplemented with 10% FBS for lysosome staining. MNP prepared using PLA covalently labeled with BODIPY FL were incubated with Cy™ 5-labeled DNA (50 μ g and 2.5 μ g, respectively) for 30 min and applied to the cells for 15 min under magnetic field as described above. The cells were washed with PBS and the medium was replaced with fresh OPTI-MEM I supplemented with 10% FBS. Cell images were obtained using three channels: green ($\lambda_{ex}/\lambda_{em}=488/492$ –519 nm), red ($\lambda_{ex}/\lambda_{em}=543/551$ –622 nm), and far red ($\lambda_{ex}/\lambda_{em}=633/640$ –754 nm) for NP, lysosomes, and plasmid DNA, respectively.

Statistical analysis

Experimental data were presented as means \pm standard deviation. The results were evaluated by regression analysis. The Student's *t* test was used to analyze the significance of individual curve slopes and compare between curves. Differences were termed significant at $P < 0.05$.

RESULTS

MNP formulation

Magnetic PLA-based nanoparticles coated with PEI ranging in particle size and magnetic properties were formulated (Fig. 2A and Table 1). Increasing the concentration of THF in the organic phase resulted in a proportional decrease in the MNP size (Fig. 2A), with the smallest (185 \pm 3 nm) and medium (240 \pm 19 nm)-sized MNP formed with 75% and 50% THF (v/v) in the organic solvent composition, whereas using chloroform alone as a solvent

resulted in larger NP of 375 ± 10 nm (s MNP, M MNP and L MNP, respectively). The efficient association of PEI as an *in situ*-formed oleate complex with MNP surface (averaging 75–92% of the initially added amount) produced a cationic surface charge of $\sim +40$ – 45 mV (Table 1). DNA binding was found to be independent of MNP size and complete in the MNP amount range studied. DNA complexation was paralleled by a decrease in zeta potential similar in all MNP types and inversely dependent on their amount (Fig. 2B). While DNA binding resulted in an increase in the MNP size on the order of 50–70 nm, no aggregation was observed in the MNP amount range studied (data not shown). The magnetite entrapment yield was comparable between MNP of different sizes (Table 1), resulting in similar magnetite loadings expressed as a weight fraction. However, since the magnetite payload is distributed in the respective formulations between MNP substantially different in size, the magnetic responsiveness of an average nanoparticle of each type differs significantly, with s MNP and L MNP possessing the lowest and the highest magnetic susceptibility, respectively (Table 1). All formulations exhibited superparamagnetic behavior showing no significant hysteresis and a remnant magnetization on the order of 0.5% of the respective saturation magnetization values, whereas nonmagnetic particles included as a control exhibited diamagnetic properties (Fig. 2C). The magnetic moment depended near-linearly on the magnetic field up to 1000 Oe, reaching 66–68% of the saturation value for all magnetic formulations, whereas a comparatively low increment in magnetization was observed on further increasing the field to 5000 Oe. The specific magnetic susceptibility of the MNP was found to be in the range of 3.0–3.3 emu/(g \times kOe) in the formulations studied, which is comparable to that of commercially available magnetic spheres with a similar iron oxide content (14)

The effect of MNP formulation parameters on gene transfer in cell culture

MNP uptake revealed similar trends in both cultured aortic smooth muscle and bovine aortic endothelial cells (A10 and BAEC, respectively). The cellular uptake depended directly on the MNP dose for the three formulation types (Fig. 3A, B). However, the cell uptake of the M MNP and s MNP formulations exhibited saturation with increased dosages, while the internalization of L MNP demonstrated a near-linear dose dependence in the entire MNP amount range studied. The GFP reporter gene expression was also directly dose dependent in both cell types, with L MNP resulting in transgene levels 1.8- to 2.7-fold higher than with smaller sized MNP in A10 and BAEC, respectively ($P < 0.01$, Fig. 3C, D). The gene expression mediated by large nonmagnetic nanoparticles included as a control was on average 10- and 35-fold lower than that of the L MNP in A10 and BAEC, respectively ($P < 0.001$, Fig. 3C, D), in accordance with their inefficient cell uptake. All types of MNP complexing DNA exhibited low toxicity in contact inhibited cells ($87 \pm 2\%$ and $96 \pm 2\%$ cell survival at the highest applied MNP dose, 5 μ g/well, in A10 and BAEC, respectively; Fig. 3E, F). Fluorescent microscopic observations confirmed the results above showing that a magnetically responsive DNA carrier is essential for achieving efficient gene transfer under the applied experimental conditions (magnetic vs. nonmagnetic nanoparticles or PEI-DNA complexes), and providing additional evidence of the significantly greater cell uptake and transfection efficiency of the larger sized MNP (see Supplemental Fig. 7).

Cell transfection by MNP in high serum conditions

L MNP that demonstrated the highest transfection efficiency in the presence of medium with low serum content (10%) were further used to study magnetically driven DNA delivery in high serum conditions (50%). Magnetic force was essential to affect MNP localization in cells in both low and high serum conditions (Fig. 4A, B). Whereas BAEC treated with L MNP for 15min or 2 h without a magnetic field (protocols 2 and 3, respectively) did not show significant cellular uptake, MNP cell treatment protocols, including 15 min of magnetic field exposure, resulted in a dose-dependent internalization of DNA-laden L MNP

that was comparably efficient with or without prior incubation of μ MNP with DNA for 2 h in serum-containing medium (protocols 1 and 4, respectively). Notably, the intracellular levels of MNP obtained with magnetic field exposure and the respective transfection efficiencies were highly dependent on the serum concentration; on average, 2.1-fold higher amounts of μ MNP were internalized per unit dose in 10% serum within 15 min ($P=0.005$), resulting in a 3-fold higher GFP expression observed with the latter at an MNP dose of 5 μ g/well. However, while higher MNP doses resulted in a reduction in GFP levels due to increasing cell toxicity in low serum conditions (results not shown), the transfection levels continued to increase with MNP dose in high serum conditions up to an MNP dose of 12 μ g/well. At this dose, the transgene expression equaled $71 \pm 14\%$ of the maximal GFP level observed in low serum conditions (Fig. 4C, D), while cell survival was $86 \pm 7\%$ relative to untreated cells (Fig. 4F). Notably, the transfection capacity of MNP was largely preserved within the entire MNP dose range after 2 h incubation in low serum conditions (Fig. 4C), whereas higher MNP amounts were necessary to achieve efficient transfection after incubation in 50% serum. Considering that the MNP uptake rate was not affected by the preincubation in high serum conditions, these results suggest that increased MNP/DNA ratios were required to maintain the gene transfer capacity of MNP-DNA complexes after an extensive exposure to serum. In agreement with these results, DNase I protection assay data demonstrated a directly dose-dependent protective effect of MNP after 30 min incubation at 37°C, whereas uncomplexed DNA was completely degraded under these conditions (see Supplemental Fig. 8).

MNP uptake and cellular localization

Internalization and trafficking of MNP were examined by confocal microscopy after incubation on a magnet of LysoTracker Red-pretreated A10 and BAEC with a formulation where magnetic μ MNP and DNA were labeled with a green and a far-red fluorescent dye, respectively. μ MNP initially bound to the plasma membrane were fully internalized by cells after 2 h, showing little DNA release at that time (Fig. 5). In both cell types, little to no colocalization of the particles with the lysosomal compartment was observed. A substantial DNA dissociation from the carrier particles localized mainly in the perinuclear space was evident 4 h after application (Fig. 5).

Growth inhibitory effects of MNP-mediated adiponectin gene transfer in cultured arterial smooth muscle cells

Cell growth inhibition after adiponectin gene transfer using MNP was studied with cultured arterial smooth muscle cells as an example of a therapeutically relevant effect. Adiponectin-encoding plasmid delivery *via* MNP resulted in a significant reduction in the A10 cell growth (Fig. 6). While increasing the dose of the MNP complexed with control plasmids (GFP with or without a promoter) resulted in a significant reduction in the viability of dividing cells (as opposed to low toxicity observed at these MNP amounts on contact-inhibited cells in another series of experiments, Fig. 3E), the effect of adiponectin transgene expression on the cell number was notably more pronounced at lower MNP amounts than with the control formulations (Fig. 6).

DISCUSSION

Here we describe a novel plasmid DNA delivery system based on biodegradable polymeric MNP with a controllable size and a high level of surface modification with PEI achieved through the self-assembly of a surface-active PEI oleate complex. This MNP formulation has some unique advantages: 1) the size of the resultant particles is readily controlled by the amount of the water miscible solvent, THF, in the binary solvent mixture used to form an organic phase; 2) high magnetic responsiveness of the MNP in the absence of magnetic

remanence is achieved due to entrapment of oleic acid-coated magnetite nanocrystals in a rigid polymeric matrix; and 3) hydrophobic PLA provides a platform for efficient MNP surface association of an ion-pair complex of PEI with oleic acid.

Magnetically driven gene transfer was demonstrated by others using iron oxide nanoparticles that were capable of complexing DNA through electrostatic interaction with PEI (5, 6). Although the concept of using magnetic force for transfection was supported by promising results in these studies (5, 6), the transfection efficiency of these iron oxide nanoparticles in high serum conditions was not investigated. Compromised colloidal stability of these iron oxide nanoparticles that aggregated on DNA complexation makes translation to the *in vivo* setting difficult (10). This indicates that differently designed formulations may be needed to optimally realize the potential of magnetically driven gene delivery. An alternative approach illustrated in the present studies provides magnetically responsive MNP with a negligible magnetic remanence (Fig. 2) through incorporation of nanocrystalline iron oxide in the solid biodegradable polymeric matrix of nanoparticles whose size is independently controlled by adjusting formulation variables during the emulsification step as described above.

Earlier studies by others explored combining the advantages of biocompatibility and stable size of solid biodegradable polymeric nanoparticles with the high transfection efficiency of PEI as a DNA complexant, using PEI-coated polylactide or polylactide-coglycolide nanoparticles (15–18). While some of these studies demonstrated cellular uptake of DNA complexed with such particles (15) and the absence of marked cell toxicity (16), the transfection rates achievable with these formulations were shown to be inferior to those of PEI-based polyplexes (16). The use of highly water-soluble unmodified PEI for the nanoparticle surface modification resulted in comparatively low surface binding yields and rapid partitioning to the external medium (17, 18), suggesting that a different strategy is required in order to achieve more efficient DNA binding and higher transfection efficiency. High levels of PEI association with MNP surface (>50 mg PEI per 200 mg PLA) were achieved in our study in one step through spontaneous generation of an amphiphilic ion-pair complex with oleate possessing strong MNP surface affinity without the need for prior chemical modification of PEI. Another important advantage of this ion pairing self-assembling strategy is that in addition to stably anchoring the DNA-complexing agent to the MNP surface, the resultant cationic surface-active complex provides colloidal stabilization of the emulsion droplets and subsequently the solidified MNP.

While the optimal nanoparticle size needs to be determined experimentally for any given therapeutic application, size limits are defined by the delivery method, the character of the target tissue, and the nanoparticle-tissue interaction. Previous studies have shown that local levels and elimination kinetics, as well as the diffusion rates of nanoparticles designed for site-specific delivery, depend critically on the carrier size favoring use of smaller sized particles (19–21). On the other hand, the efficient magnetic concentration of the particles at the target site requires sufficient magnetic responsiveness achievable with MNP above a certain size threshold. Thus, the ability to control the particle size by adjusting the formulation variables is essential for successful *in vivo* use. The size of the PLA-based MNP formulated and characterized in our study can be controlled by adjusting the ratio of the organic solvents used in the emulsification step. The inclusion of a water-miscible solvent in the organic phase results in a decrease in particle size as its gradient-driven distribution into the aqueous medium provides additional energy resulting in formation of smaller sized nanospheres (22). A similar approach with a binary organic solvent mixture where acetone was used as a water-miscible component has been used for polylactide nanoparticle size control (23, 24). Acetone, however, is a poor suspending medium for oleic acid-stabilized nanocrystalline magnetite; therefore, an alternative solvent, THF, which either alone or in

combination with chloroform maintains the stability of the ferrofluid (data not shown) and is a good solvent to PLA, as well as PEI oleate ion-pair complex, was used in this study.

The magnetic responsiveness of MNP was sufficient for their rapid concentration on the surface of cells in the presence of a viscous medium containing 50% serum with subsequent binding and cell entry (Fig. 4B). Our results show that efficient cell internalization and transfection under the applied conditions were achievable only by combining the use of a magnetic carrier and the presence of a magnetic field, as only marginal transfection was observed in the absence of magnetic exposure (Fig. 4C, D) or with control nonmagnetic nanoparticles (Fig. 3C, D).

Whereas MNP of three different sizes displayed equally effective DNA binding, similar zeta potentials, and magnetic concentration efficiencies (Fig. 2, Table 1), the larger sized MNP exhibited a distinct near-linear pattern of cell uptake, showing no saturation in the dose range studied and transfection rates significantly greater than those of the smaller sized MNP in confluent cell culture (Fig. 3A–D). This agrees with the findings by Rejman *et al.* (25), who observed a shift in the uptake mechanism with the nanoparticle size between 200 nm and 500 nm and showed that larger sized nanoparticles did not localize in the lysosomal compartment after cell entry in accord with our confocal microscopy results. The superior gene transfer rates observed with the larger MNP (375±10 nm) therefore may be associated with the size dependency of the MNP uptake and intracellular processing (26).

The larger sized MNP further used to study the effect of serum-containing medium on gene transfer showed high transfection rates after 15 min magnetic field exposure as opposed to negligible transfection observed in the absence of magnetic field after either 15 min or 2 h incubation, in accordance with the respective nanoparticle internalization rates (Fig. 4C, D). The transfection capacity of the MNP was practically unaffected by a 2 h incubation in the presence of 10% serum (Fig. 4C) and was significantly preserved by using higher MNP to DNA ratios in high serum conditions (Fig. 4D), suggesting that the MNP amount needs to be optimized to provide effective DNA binding and protection in biological conditions. At the same time, this binding was reversible in the cell interior per our confocal microscopy results (Fig. 5) showing that DNA was released from the MNP after their cell entry and transport to the perinuclear zone (4 h).

The ability to overcome limited transfection efficiencies in the presence of serum nucleases and deliver DNA in quiescent cells with a nonviral vector demonstrated in this study is critical for many clinical applications. It is of particular interest for cardiovascular therapy that effective transfection of vascular cells is achievable after a short exposure of cells to a transgene binding formulation in view of the rapid elimination of PLA-based MNP from the arterial tissue demonstrated in previous studies (19). It is of note that the high transfection rates were achieved in quiescent cells at increasing MNP to DNA ratios without decreasing the cell viability below 85% (Figs. 3, 4), in contrast to the results reported by Krötz *et al.* for endothelial cells transfected using PEI-containing iron oxide nanoparticle formulations (7). However, a reduction in the viable cell number with increasing MNP dose was observed in dividing smooth muscle cells (Fig. 6). This effect on cell viability was associated with complexes rather than the gene product, as it was evident with MNP complexed with either a functional GFP plasmid or a plasmid without a promoter and apparently is explained by facilitated nuclear entry of PEI-coated nanoparticles in proliferating cells, which is normally prevented by the nuclear membrane in the absence of mitosis. The cytotoxicity of PEI is well documented (27, 28) and has been shown to depend on the concentration of PEI in the cell nucleus, where it may interfere with critical cell functions (29). This differential effect on dividing cells is potentially of interest considering treatment of proliferative disorders, such as restenosis. However, we also showed that a strong growth inhibition of smooth

muscle cells cultured in PDGF-BB-supplemented medium was achievable with lower doses of MNP combined with adiponectin-encoding plasmid in the absence of significant nonspecific cell toxicity. The mechanism of the observed growth inhibitory effect apparently involves blocking interaction of the growth factor with its receptor by PDGF-BB binding with adiponectin ($K_d=38\pm6$ pM), as shown by Wang *et al.* (30). Previous studies using systemic adenoviral delivery of adiponectin in the animal model of restenosis showed a significant antirestenotic effect (31) that apparently was associated with the smooth muscle cell growth inhibition also observed in our study. This study is the first to examine nonviral, magnetically driven gene delivery of adiponectin using biodegradable MNP and provides a basis for exploring the therapeutic potential of this approach in future *in vivo* studies.

Magnetically driven local delivery of pharmaceutical loaded nanoparticles to tumors has been reported both experimentally (32, 33) and clinically (34, 35) using direct positioning of a fixed magnet over the targeting site for localization. The MNP reported in the present study could be used for magnetically driven gene delivery *in vivo* with a comparable approach, or targeting could be achieved to ferromagnetic implants, such as stents, by the use of a uniform magnetic field with MNP localization to high field gradients (36) on stent struts, as shown in feasibility studies by our group (37).

CONCLUSIONS

Biodegradable magnetite-laden MNP were formulated with controllable size and surface modification with PEI oleate ion-pair complex. As a result, these MNP efficiently bound, protected, and delivered plasmid DNA in the presence of serum and allowed for high transfection efficiency in contact-inhibited cultured vascular cells. In addition to reporter studies, a therapeutically relevant and specific growth inhibitory effect was achievable in smooth muscle cells after magnetically driven transfection with adiponectin-encoding plasmid DNA. The results of this study show that biodegradable, polymer-based MNP coated with PEI address a number of important challenges to successful nonviral gene delivery, and in combination with a magnetic guidance strategy, may be an important candidate delivery system for site-specific gene therapy applications.

Acknowledgments

The authors thank Ms. Ashleigh Hahn from the Children's Hospital of Philadelphia for assistance in performing confocal microscopy studies and Dr. Neelima Shah from the University of Pennsylvania for help with the TEM studies. This research was supported by National Institutes of Health grant HL72108, The Nanotechnology Institute, and the William J. Rashkind Endowment of the Children's Hospital of Philadelphia.

REFERENCES

1. Barry ME, Pinto-Gonzalez D, Orson FM, McKenzie GJ, Petry GR, Barry MA. Role of endogenous endonucleases and tissue site in transfection and CpG-mediated immune activation after naked DNA injection. *Hum. Gene Ther.* 1999; 10:2461–2480. [PubMed: 10543612]
2. Lechardeur D, Sohn KJ, Haardt M, Joshi PB, Monck M, Graham RW, Beatty B, Squire J, O'Brodovich H, Lukacs GL. Metabolic instability of plasmid DNA in the cytosol: a potential barrier to gene transfer. *Gene Ther.* 1999; 6:482–497. [PubMed: 10476208]
3. Dean DA, Strong DD, Zimmer WE. Nuclear entry of nonviral vectors. *Gene Ther.* 2005; 12:881–890. [PubMed: 15908994]
4. Rolland A. Nuclear gene delivery: the Trojan horse approach. *Expert Opin. Drug Deliv.* 2006; 3:1–10. [PubMed: 16370936]
5. Scherer F, Anton M, Schillinger U, Henke J, Bergemann C, Krüger A, Gansbacher B, Plank C. Magnetofection: enhancing and targeting gene delivery by magnetic force in vitro and in vivo. *Gene Ther.* 2002; 9:102–109. [PubMed: 11857068]

6. Plank C, Scherer F, Schillinger U, Bergemann C, Anton M. Magnetofection: enhancing and targeting gene delivery with superparamagnetic nanoparticles and magnetic fields. *J. Liposome Res.* 2003; 13:29–32. [PubMed: 12725725]
7. Krötz F, Sohn HY, Gloe T, Plank C, Pohl U. Magnetofection potentiates gene delivery to cultured endothelial cells. *J. Vasc. Res.* 2003; 40:425–434. [PubMed: 14530599]
8. Plank C, Anton M, Rudolph C, Rosenecker J, Krötz F. Enhancing and targeting nucleic acid delivery by magnetic force. *Expert Opin. Biol. Ther.* 2003; 3:745–758. [PubMed: 12880375]
9. Plank C, Schillinger U, Scherer F, Bergemann C, Remy JS, Krötz F, Anton M, Lausier J, Rosenecker J. The magnetofection method: using magnetic force to enhance gene delivery. *Biol. Chem.* 2003; 384:737–747. [PubMed: 12817470]
10. Xenariou S, Griesenbach U, Ferrari S, Dean P, Scheule RK, Cheng SH, Geddes DM, Plank C, Alton EW. Using magnetic forces to enhance non-viral gene transfer to airway epithelium in vivo. *Gene Ther.* 2006; 13:1545–1552. [PubMed: 16738690]
11. Dunlap DD, Maggi A, Soria MR, Monaco L. Nanoscopic structure of DNA condensed for gene delivery. *Nucleic Acids Res.* 1997; 25:3095–3101. [PubMed: 9224610]
12. Quintanar-Guerrero D, Allémann E, Fessi H, Doelker E. Preparation techniques and mechanisms of formation of biodegradable nanoparticles from preformed polymers. *Drug Dev. Ind. Pharm.* 1998; 24:1113–1128. [PubMed: 9876569]
13. Ferrari ME, Rusalov D, Enas J, Wheeler CJ. Trends in lipoplex physical properties dependent on cationic lipid structure, vehicle and complexation procedure do not correlate with biological activity. *Nucleic Acids Res.* 2001; 29:1539–1548. [PubMed: 11266556]
14. Häfeli UO, Ciocan R, Dailey JP. Characterization of magnetic particles and microspheres and their magnetophoretic mobility using a digital microscopy method. *Eur. Cell. Mater.* 2002; 3(Suppl. 2): 24–27.
15. Bivas-Benita M, Romeijn S, Junginger HE, Borchard G. PLGA-PEI nanoparticles for gene delivery to pulmonary epithelium. *Eur. J. Pharm. Biopharm.* 2004; 58:1–6. [PubMed: 15207531]
16. Kim IS, Lee SK, Park YM, Lee YB, Shin SC, Lee KC, Oh IJ. Physicochemical characterization of poly(l-lactic acid) and poly(d,l-lactide-co-glycolide) nanoparticles with polyethylenimine as gene delivery carrier. *Int. J. Pharm.* 2005; 298:255–262. [PubMed: 15941631]
17. Messai I, Munier S, Ataman-Önal Y, Verrier B, Delair T. Elaboration of poly(ethyleneimine) coated poly(d,l-lactic acid) particles. Effect of ionic strength on the surface properties and DNA binding capabilities. *Colloids Surf. B Biointerfaces.* 2003; 32:293–305.
18. Trimaille T, Pichot C, Delair T. Surface functionalization of poly(d,l-lactic acid) nanoparticles with poly(ethyleneimine) and plasmid DNA by the layer-by-layer approach. *Colloids Surf. A Physicochem. Eng. Asp.* 2003; 221:39–48.
19. Fishbein I, Chorny M, Banai S, Levitzki A, Danenberg HD, Gao J, Chen X, Moerman E, Gati I, Goldwasser V, Golomb G. Formulation and delivery mode affect disposition and activity of tyrphostin-loaded nanoparticles in the rat carotid model. *Arterioscler. Thromb. Vasc. Biol.* 2001; 21:1434–1439. [PubMed: 11557668]
20. Song CX, Labhasetwar V, Murphy H, Qu X, Humphrey WR, Shebuski RJ, Levy RJ. Formulation and characterization of biodegradable nanoparticles for intravascular local drug delivery. *J. Control Release.* 1997; 43:197–212.
21. Kuhn SJ, Hallahan DE, Giorgio TD. Characterization of superparamagnetic nanoparticle interactions with extracellular matrix in an in vitro system. *Ann. Biomed. Eng.* 2006; 34:51–58. [PubMed: 16477503]
22. Quintanar-Guerrero D, Allemann E, Doelker E, Fessi H. A mechanistic study of the formation of polymer nanoparticles by the emulsification-diffusion technique. *Colloid Polym. Sci.* 1997; 275:640–647.
23. Chorny M, Fishbein I, Danenberg HD, Golomb G. Lipophilic drug loaded nanospheres prepared by nano-precipitation: effect of formulation variables on size, drug recovery and release kinetics. *J. Control Release.* 2002; 83:389–400. [PubMed: 12387947]
24. Wehrle P, Magenheimer B, Benita S. The influence of process parameters on the PLA nanoparticle size distribution, evaluated by means of factorial design. *Eur. J. Pharm. Biopharm.* 1995; 41:19–26.

25. Rejman J, Oberle V, Zuhorn IS, Hoekstra D. Size-dependent internalization of particles via the pathways of clathrin- and caveolae-mediated endocytosis. *Biochem. J.* 2004; 377:159–169. [PubMed: 14505488]
26. Medina-Kauwe LK, Xie J, Hamm-Alvarez S. Intracellular trafficking of nonviral vectors. *Gene Ther.* 2005; 12:1734–1751. [PubMed: 16079885]
27. Brownlie A, Uchegbu IF, Schatzlein AG. PEI-based vesicle-polymer hybrid gene delivery system with improved biocompatibility. *Int. J. Pharm.* 2004; 274:41–52. [PubMed: 15072781]
28. Moghimi SM, Symonds P, Murray JC, Hunter AC, Debska G, Szewczyk A. A two-stage poly(ethylenimine)-mediated cytotoxicity: implications for gene transfer/therapy. *Mol. Ther.* 2005; 11:990–995. [PubMed: 15922971]
29. Clamme JP, Krishnamoorthy G, Mely Y. Intracellular dynamics of the gene delivery vehicle polyethylenimine during transfection: investigation by two-photon fluorescence correlation spectroscopy. *Biochim. Biophys. Acta.* 2003; 1617:52–61. [PubMed: 14637019]
30. Wang Y, Lam KS, Xu JY, Lu G, Xu LY, Cooper GJ, Xu A. Adiponectin inhibits cell proliferation by interacting with several growth factors in an oligomerization-dependent manner. *J. Biol. Chem.* 2005; 280:18341–18347. [PubMed: 15734737]
31. Matsuda M, Shimomura I, Sata M, Arita Y, Nishida M, Maeda N, Kumada M, Okamoto Y, Nagaretani H, Nishizawa H, et al. Role of adiponectin in preventing vascular stenosis. The missing link of adipo-vascular axis. *J. Biol. Chem.* 2002; 277:37487–37491. [PubMed: 12138120]
32. Alexiou C, Arnold W, Klein RJ, Parak FG, Hulin P, Bergemann C, Erhardt W, Wagenpfeil S, Lübke AS. Locoregional cancer treatment with magnetic drug targeting. *Cancer Res.* 2000; 60:6641–6648. [PubMed: 11118047]
33. Goodwin SC, Bittner CA, Peterson CL, Wong G. Single-dose toxicity study of hepatic intra-arterial infusion of doxorubicin coupled to a novel magnetically targeted drug carrier. *Toxicol. Sci.* 2001; 60:177–183. [PubMed: 11222884]
34. Lemke AJ, Senfft von Pilsach MI, Lübke A, Bergemann C, Riess H, Felix R. MRI after magnetic drug targeting in patients with advanced solid malignant tumors. *Eur. Radiol.* 2004; 14:1949–1955. [PubMed: 15300401]
35. Lübke AS, Bergemann C, Riess H, Schriever F, Reichardt P, Possinger K, Matthias M, Dorken B, Herrmann F, Gurtler R, et al. Clinical experiences with magnetic drug targeting: a phase I study with 4'-epidoxorubicin in 14 patients with advanced solid tumors. *Cancer Res.* 1996; 56:4686–4693. [PubMed: 8840985]
36. Yellen BB, Hovorka O, Friedman G. Arranging matter by magnetic nanoparticle assemblers. *Proc. Natl. Acad. Sci. U. S. A.* 2005; 102:8860–8864. [PubMed: 15956215]
37. Yellen BB, Chorny M, Fishbein I, Dai N, Ottey A, Klingerman C, Alferiev I, Nyanguile O, Friedman G, Levy RJ. Site specific gene delivery using magnetic forces to localize adenoviral vector-magnetic nanoparticle complexes to stented arterial segments. *Circulation.* 2005; 112:653. (abstr.).

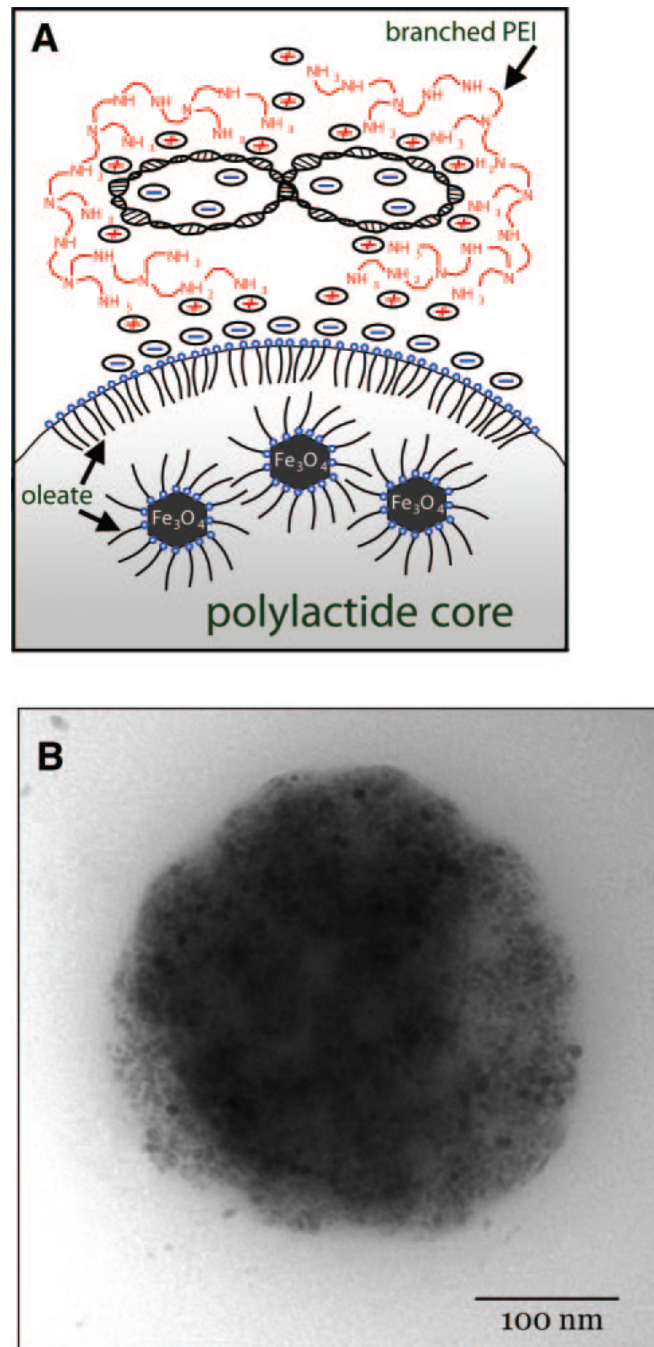


Figure 1. Magnetic nanoparticles (MNP) with surface complexed DNA. *A*) Schematically shown structure of a plasmid DNA-MNP complex based on polylactide plus oleate-coated iron oxide. MNP surface modification with polyethylenimine (PEI) *via* ion pairing with oleate enables formation of MNP-DNA complexes. For the sake of simplicity, only primary and a part of the secondary amines of branched PEI are shown protonated on the scheme. PEI complexation of plasmid DNA results in formation of compact condensates (11). *B*) Transmission electron microscopy of MNP was performed after negative staining with 2% uranyl acetate (FEI Tecnai G2 electron microscope, Eindhoven, Netherlands). Note the

small size and the large number of individual oleic acid-coated magnetite grains distributed in the MNP polymeric matrix.

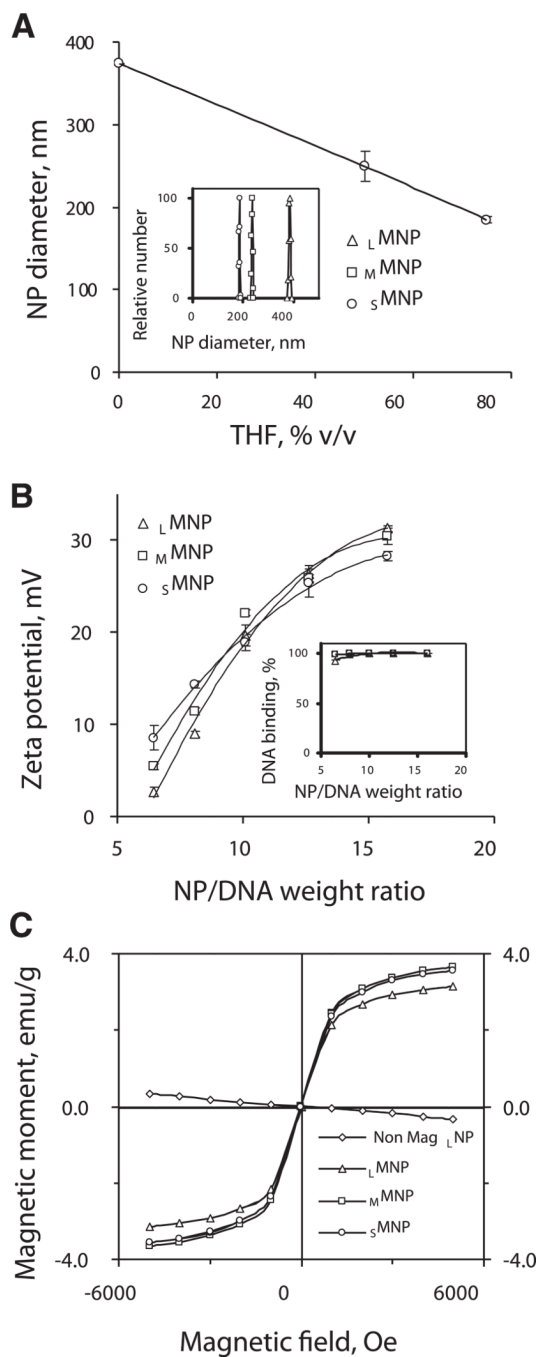


Figure 2.

Structural and physical characterization of MNP. *A*) MNP size as a function of THF amount in the organic phase. Insert shows the size distribution of the MNP. *B*) Zeta potential of DNA-complexing MNP as a function of the MNP/DNA weight ratio. Insert presents the effect of MNP/DNA weight ratio on DNA binding determined by PicoGreen assay. Varying MNP amounts were applied to 0.1 μ g DNA and the unbound DNA was measured fluorimetrically ($\lambda_{ex}/\lambda_{em}=485$ nm/530 nm). *C*) Magnetization curves of MNP formulations (125 μ g samples). Note the absence of remanence (superparamagnetism) exhibited by the three types of MNP and the diamagnetic behavior of nonmagnetic nanoparticles measured as a control in an equivalent sample amount. Error bars indicate s_D .

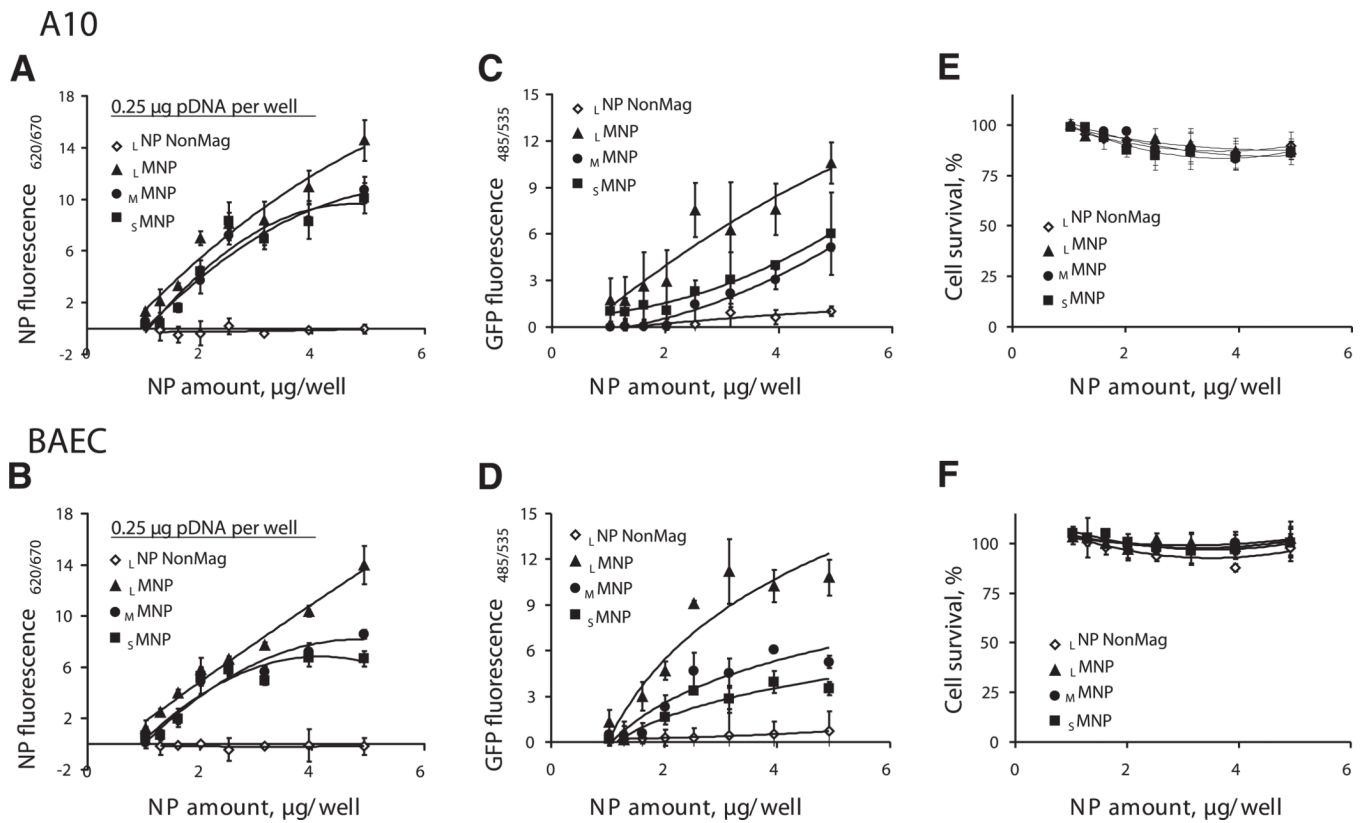
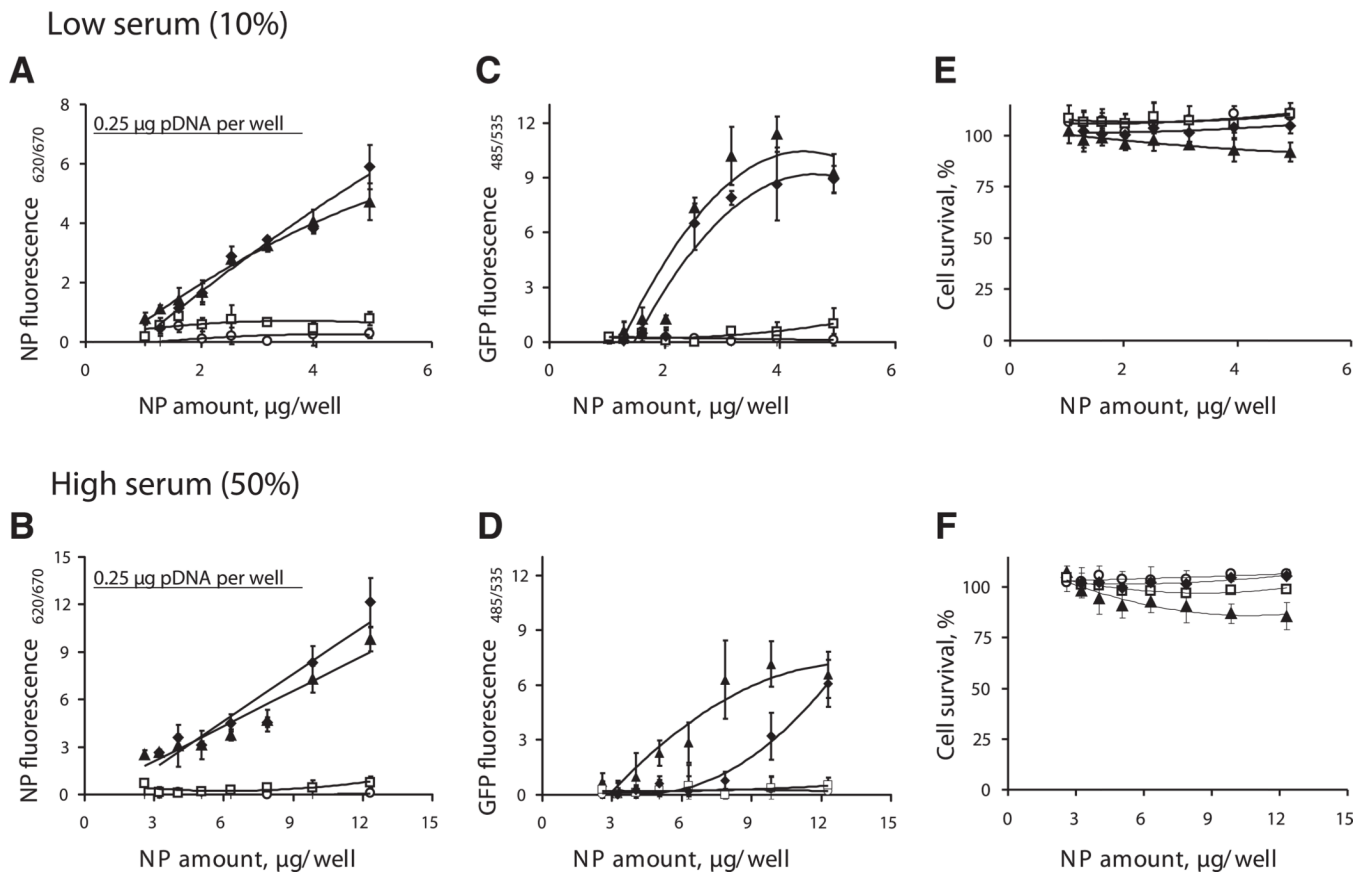


Figure 3.

MNP uptake, GFP reporter expression, and cell viability in smooth muscle cells (A10) and bovine aortic endothelial cells (BAEC) (top and bottom rows, respectively) treated with three types of DNA complexing MNP, and nonmagnetic nanoparticles included as a control. MNP (1–5 μg per well) were incubated with DNA (0.25 $\mu\text{g}/\text{well}$) for 30 min and added to cells for 15 min under magnetic field. The uptake of MNP fluorescently labeled with PLA-BODIPY_{650/665} was determined fluorimetrically ($\lambda_{\text{ex}}/\lambda_{\text{em}}$ 620 nm/670 nm) in A10 cells and BAEC (A and B, respectively) after 24 h. Note the insignificant internalization of nonmagnetic nanoparticles compared with the MNP formulations. GFP expression of A10 (C) and BAEC (D) was determined fluorimetrically (485 nm/535 nm) in live cells 48 h post-treatment. Note the significantly higher transgene levels achieved with L MNP in both cell types compared with smaller sized MNP ($P < 0.01$) and the marginal transfection mediated by nonmagnetic nanoparticles under the applied conditions ($P < 0.001$ vs. magnetic L MNP in both cell types). Viability of A10 (E) and BAEC (F) was determined 72 h post-treatment using the AlamarBlue assay. Error bars indicate s_{D} .

**Figure 4.**

MNP uptake (*A, B*), GFP reporter expression (*C, D*), and cell viability (*E, F*) in BAEC treated with DNA (0.25 μg/well) complexed with \perp MNP and applied to cells in low and high serum conditions (10% and 50% serum, respectively). (▲) Protocol 1: complexes applied under magnetic field for 15 min; (○) protocol 2: complexes applied without a magnetic field for 15 min; (□) protocol 3: complexes applied without a magnetic field for 2 h; (◆) protocol 4: complexes preincubated in the serum-containing medium for 2 h at 37°C and applied to cells under magnetic field for 15 min. Error bars indicate *SD*.

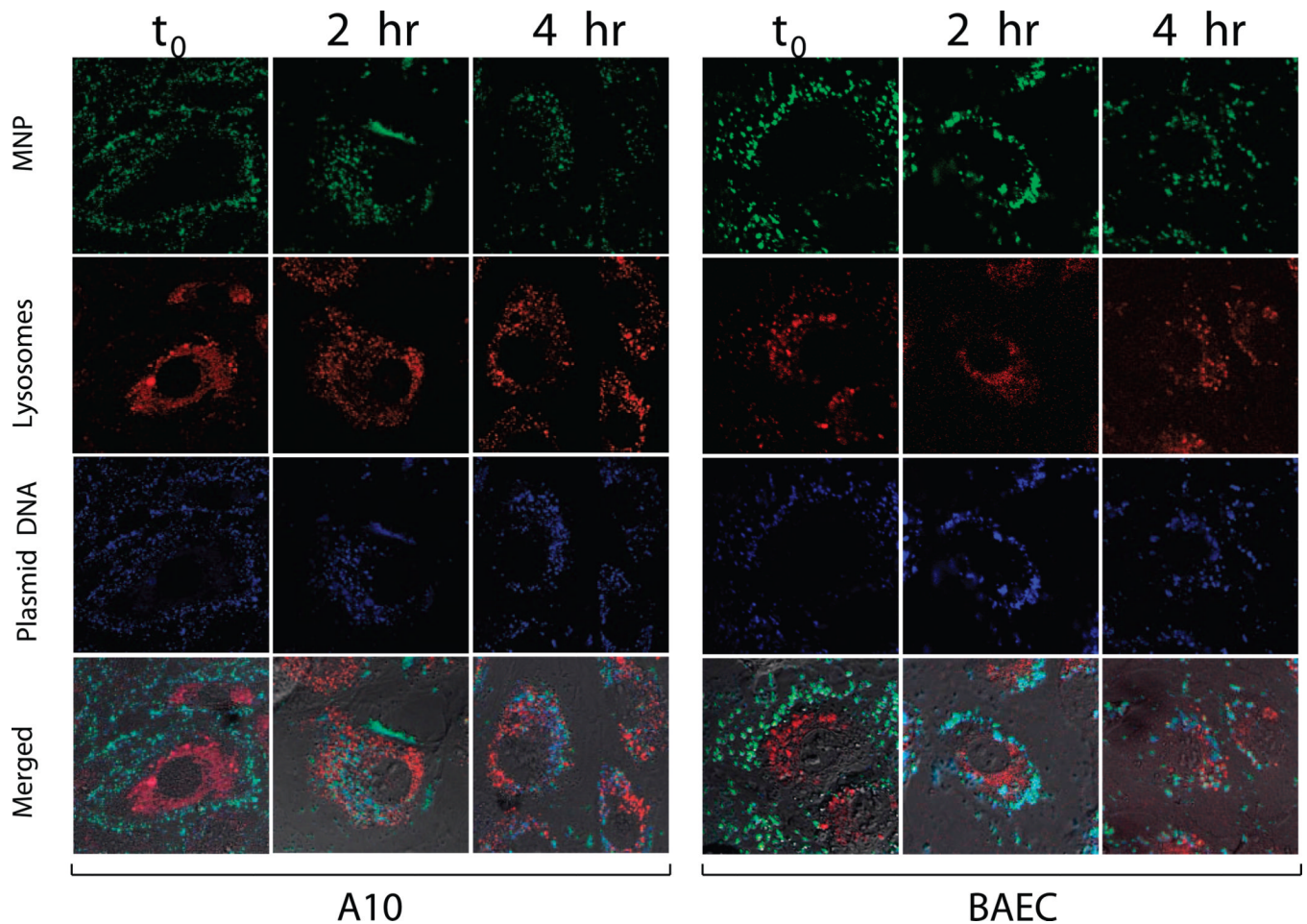


Figure 5.

Internalization and trafficking of fluorescently labeled L MNP-DNA complexes examined by confocal microscopy in A10 (left panel) and BAEC (right panel). L MNP prepared using polylactide covalently labeled with BODIPY (FL) were incubated with CyTM 5-labeled DNA (5 μ g and 0.25 μ g, respectively) for 30 min and applied to cells for 15 min under magnetic field. One hour before applying MNP-DNA complexes, cells were pretreated with Lysotracker Red at a concentration of 50 nM in DMEM supplemented with 10% FBS for lysosome staining. Cells images were obtained using three channels: green ($\lambda_{ex}/\lambda_{em}$ =488/492–519 nm), red ($\lambda_{ex}/\lambda_{em}$ =543/551–622 nm), and far red ($\lambda_{ex}/\lambda_{em}$ =633/640–754 nm) for MNP, lysosomes, and DNA, respectively. Note the cellular uptake of the complexes complete after 2 h, with little colocalization with the lysosomal compartment, and the substantial DNA dissociation from the carrier MNP in the cytosol 4 h after application.

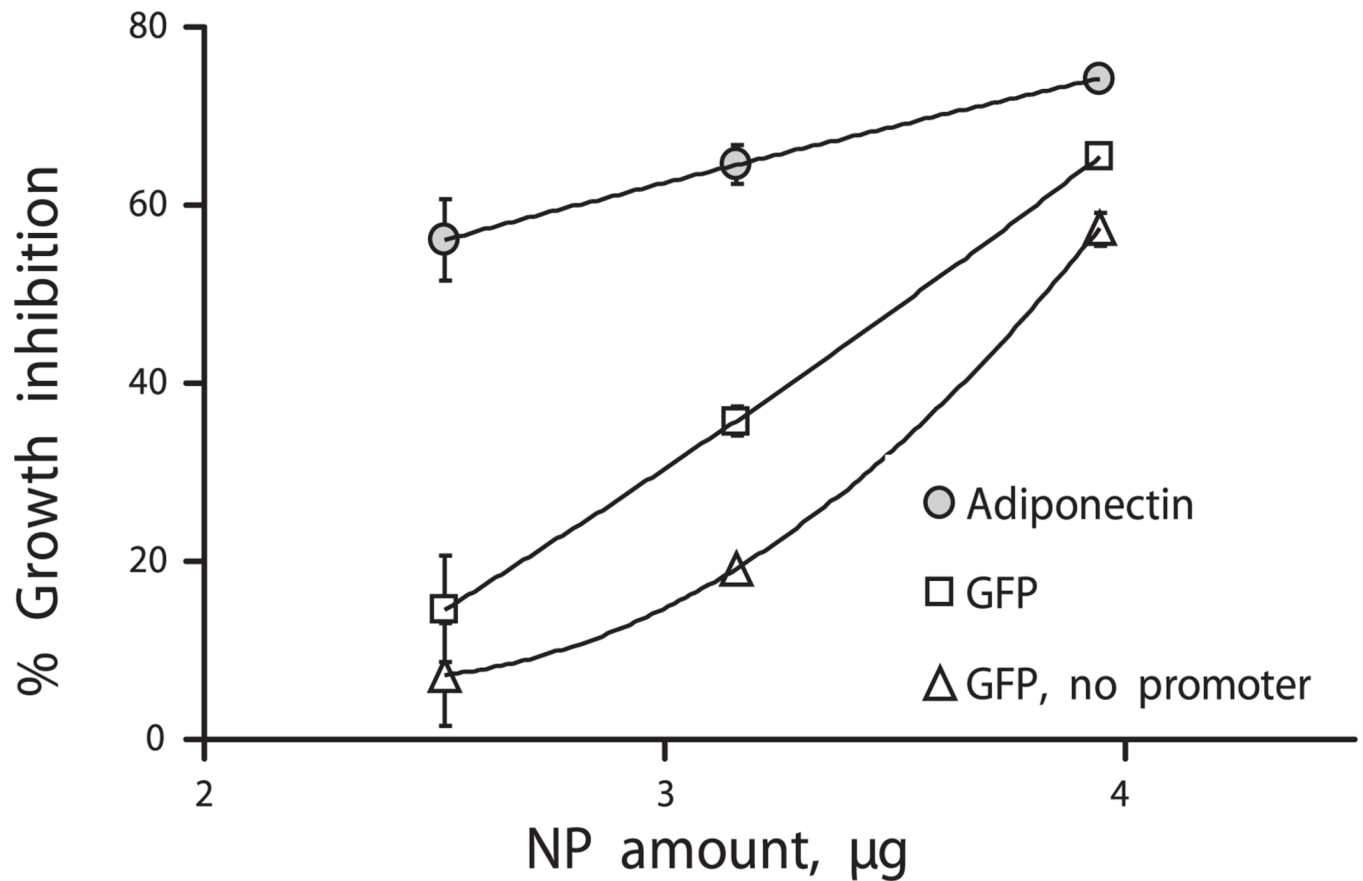


Figure 6.

Inhibitory effect of MNP-mediated adiponectin gene transfer on the growth factor-induced (PDGF-BB) proliferation of cultured smooth muscle cells (A10). Culture medium (DMEM) was supplemented with PDGF-BB at a concentration of 10 ng/ml and 2% of FBS. Growth inhibition of A10 seeded at 30% confluence mediated by adiponectin-encoding L^{MNP} -DNA complexes (0.25 μg DNA/well) was measured in comparison to control complexes prepared with plasmids for GFP and GFP without a promoter.

TABLE 1Characteristics of PLA-based MNP coated with PEI^a

NP formulation	_L MNP	_M MNP	_S MNP
Magnetite entrapment yield, %	95.5 ± 2.2	91.6 ± 3.7	94.5 ± 5.9
Magnetite loading, % w/w	10.4 ± 0.2	10.0 ± 0.4	10.3 ± 0.6
Magnetic susceptibility, memu/(kOe×10 ¹⁵ MNP)	138.9 ± 1.2	39.4 ± 0.7	16.9 ± 0.7
Zeta potential, mV	+40.3 ± 2.2	+41.6 ± 0.7	+45.1 ± 0.5
PEI binding efficiency, %	75.2 ± 15.4	92.1 ± 18.1	89.2 ± 3.5

^a A comparison between large, medium, and small NP (375 ± 10 nm, 240 ± 19 nm, and 185 ± 3 nm, respectively).